Electronic Supplementary Information

A nano interlayer spacing and rich defect 1T-MoS_2 as cathode for superior performance aqueous zinc-ion batteries

Chengyan Cai,‡[a] Zengren Tao,‡[a] Yuanfei Zhu,[a] Yuanming Tan,[a] Anding Wang,[a] Haiyun Zhou [a,*] and Yangyi Yang [a,*]

[a]School of Materials Science and Engineering, Sun Yat-sen University Test Center, Sun Yat-sen University, Guangzhou, 510275,China.

E-mail: zhouhy@mail.sysu.edu.cn; cesyyy@mail.sysu.edu.cn

‡ These authors contributed equally to this work.

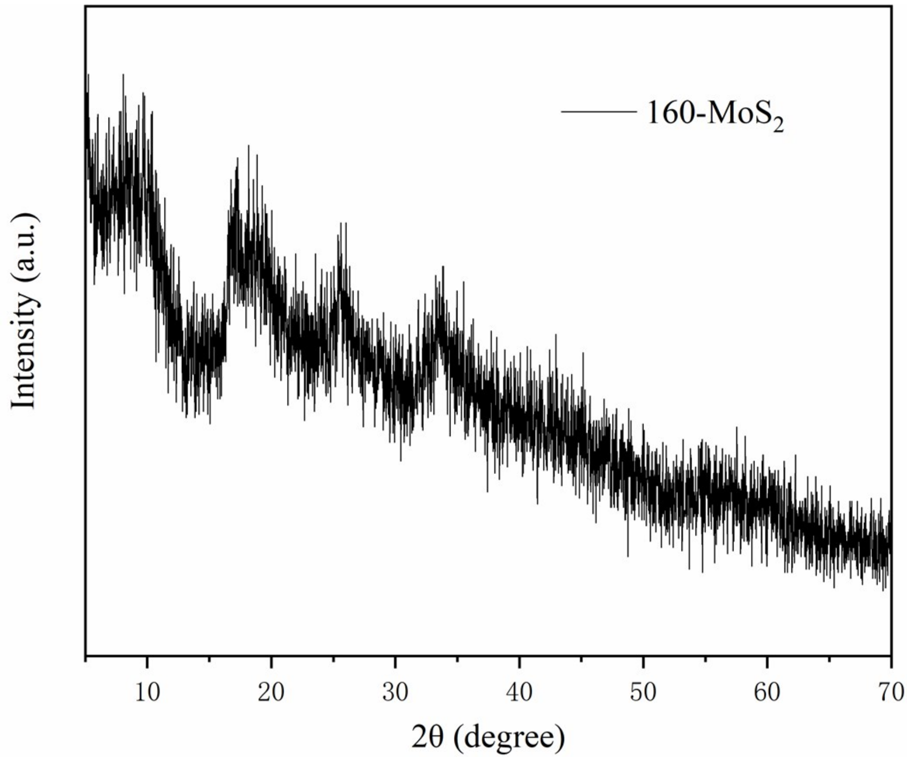

Fig. S1. XRD pattern of 160-MoS_2.

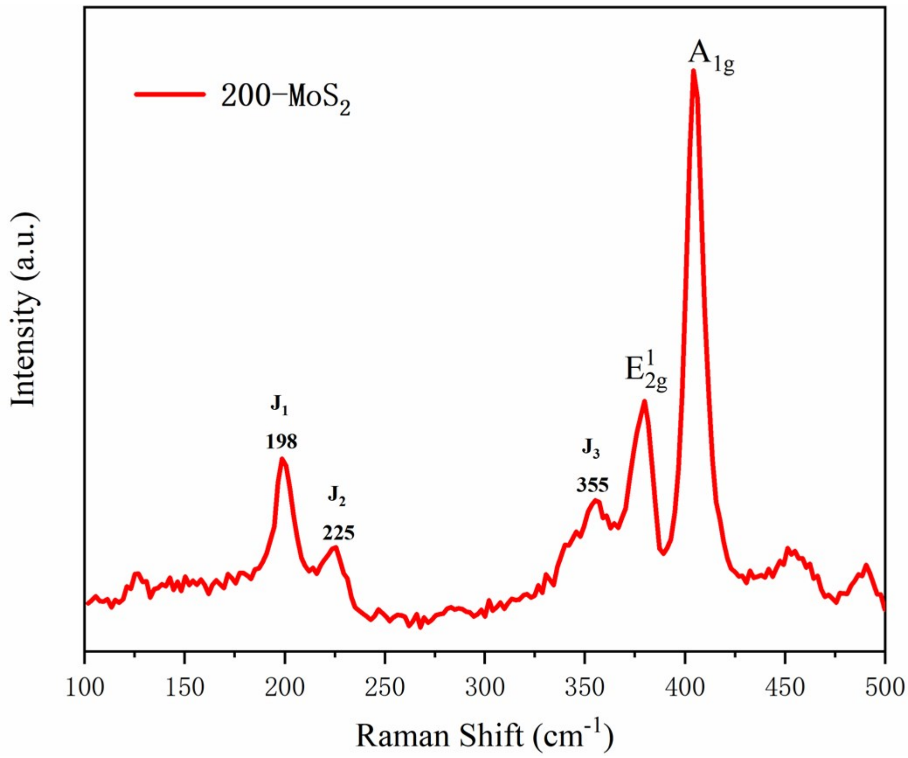

Fig. S2. Raman spectra of 200-MoS_2.

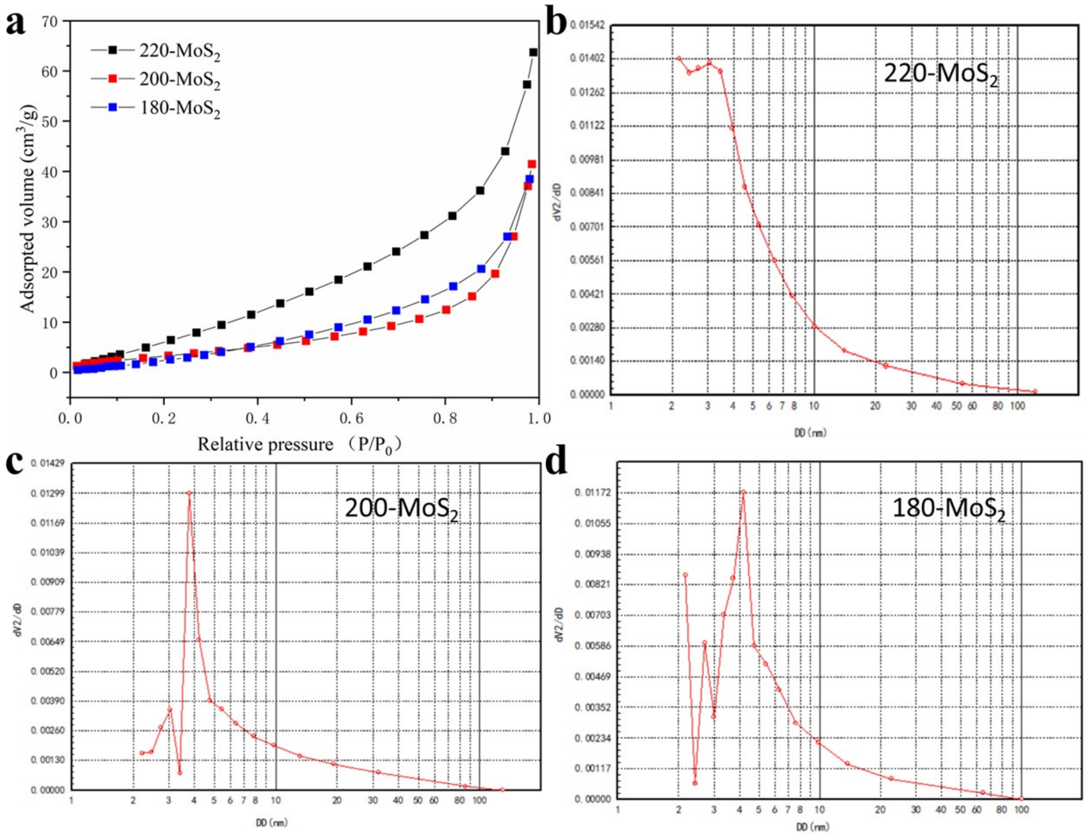

Fig. S3. (a) MoS_2 adsorption isotherms at different temperatures, pore volume-pore size distribution curve of (b) 220-MoS_2, (c) 200-MoS_2, (d) 180-MoS_2.

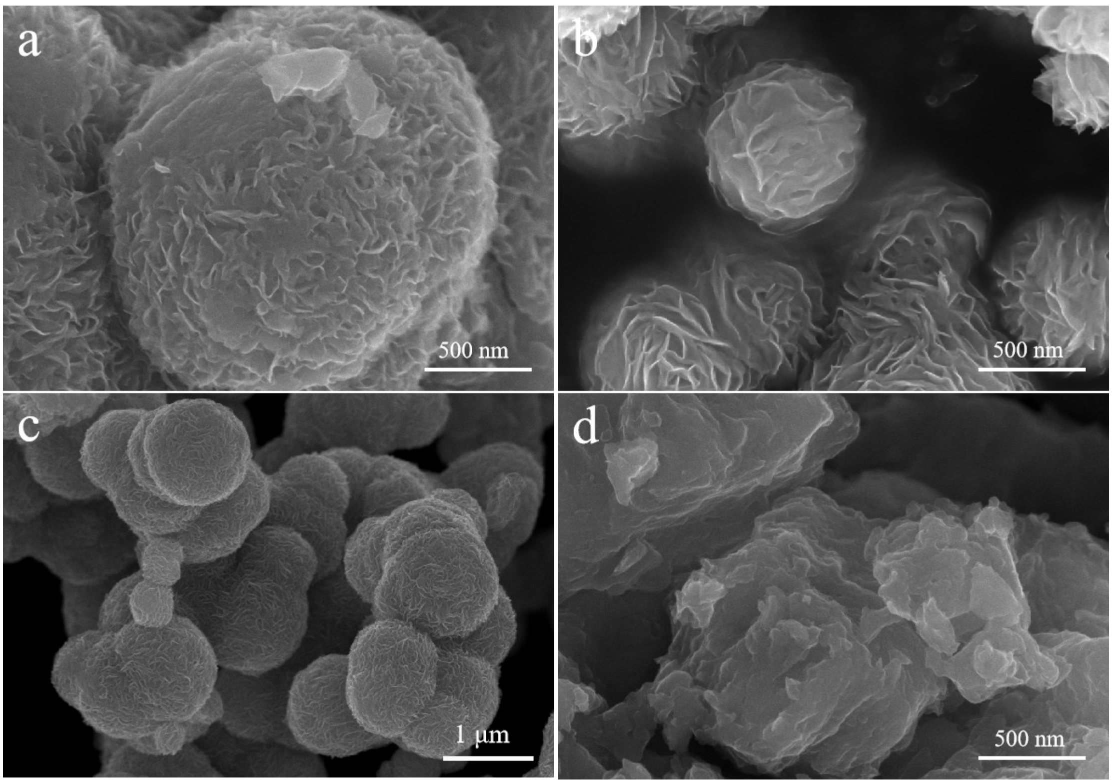

Fig. S4. TEM images of (a) 220-MoS_2, (b) 200-MoS_2, (c) 180-MoS_2, (d) 160-MoS_2.

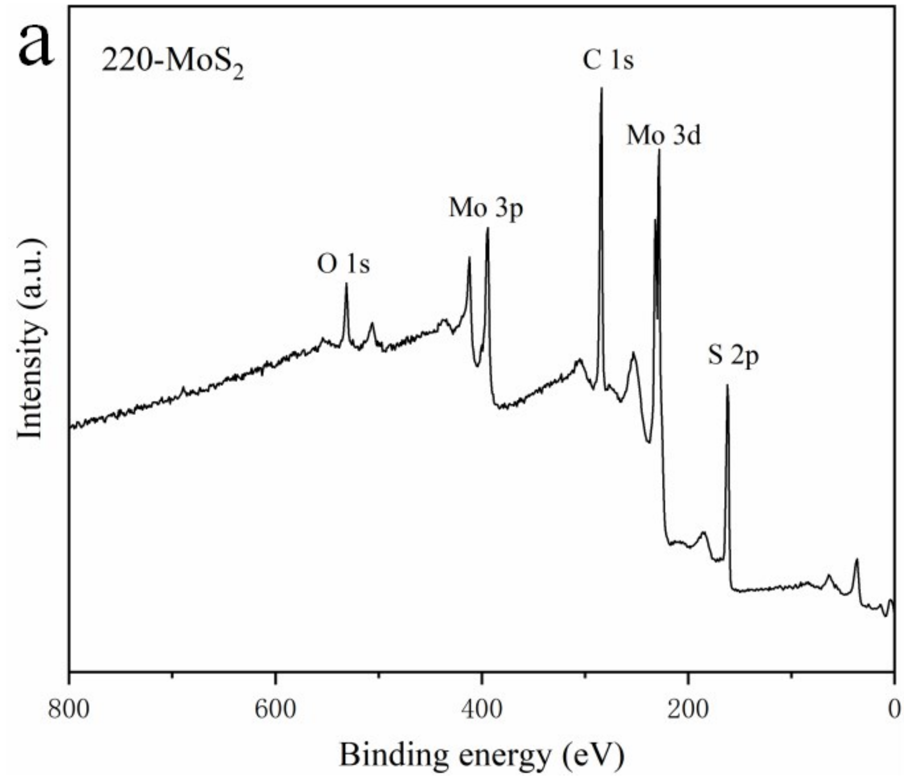
a
220-MoS2
C 1s
Mo 3d
Mo 3p
O 1s
S 2p
Intensity (a.u.)
800
600
400
200
0
Binding energy (eV)

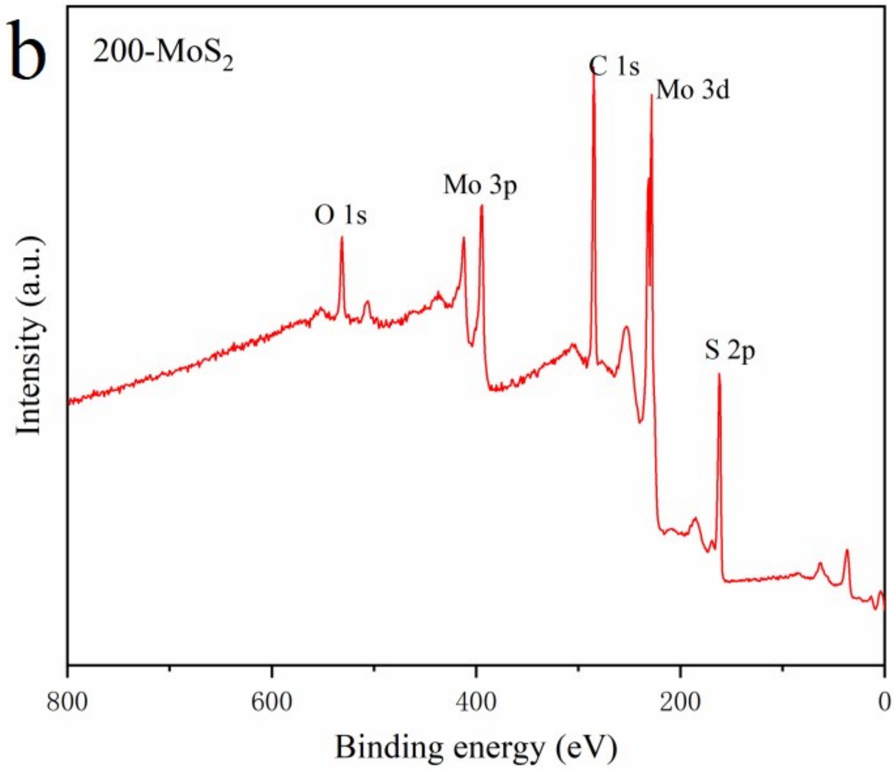
b
200-MoS2
C 1s
Mo 3d
Mo 3p
O 1s
S 2p
Intensity (a.u.)
800
600
400
200
0
Binding energy (eV)

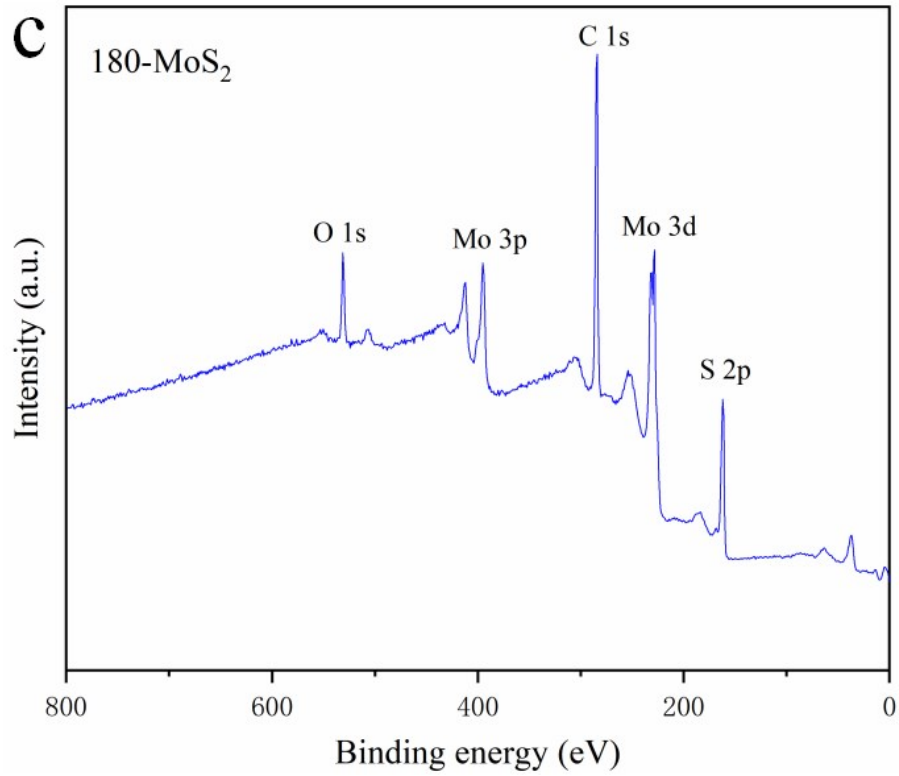

Fig. S5. Full range XPS spectra of (a) 220-MoS_2, (b) 200-MoS_2, (c) 180-MoS_2.

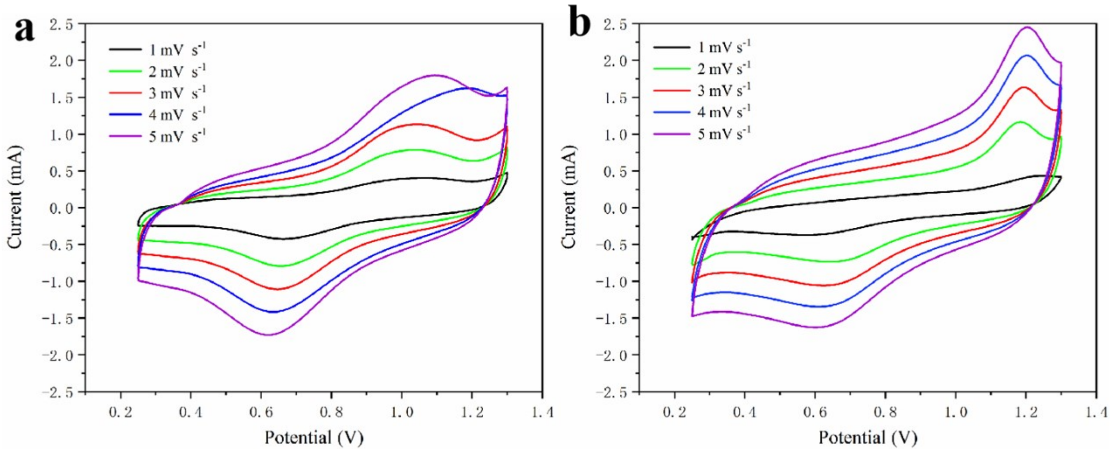

Fig. S6. (a) CV curves of 220-MoS_2 at different scan rates, (b) CV curves of 180-MoS_2 at different scan rates.

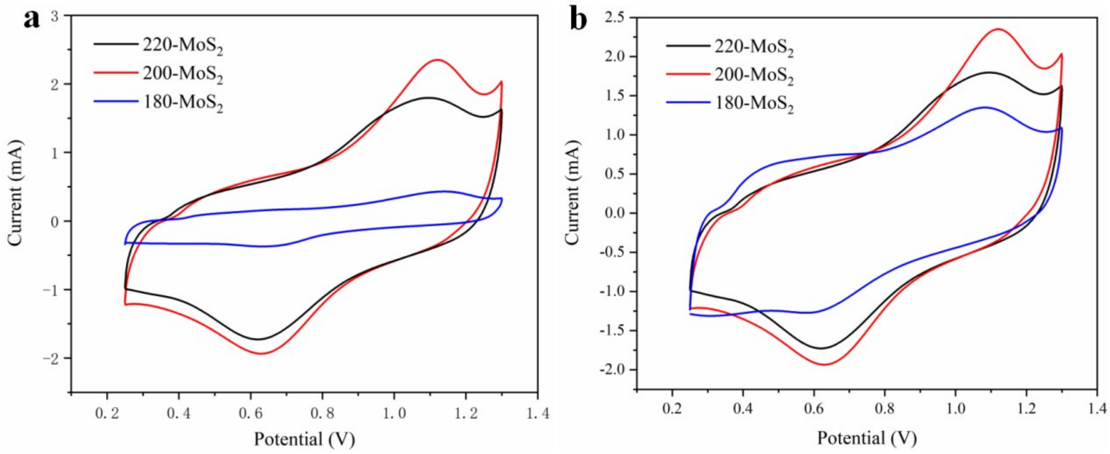

Fig. S7. (a) CV curves of 1 mV s^{-1} at different temperature, (b) CV curves of 5 mV s^{-1} at different temperature.

At the same scan rates, 200-MoS_2 has a higher redox peak. The CV curve shape of 200-MoS_2 at different scanning speeds is similar, indicating that it has excellent cycle stability. By contrast, the large difference in the shape of the CV curve of 180-MoS_2 at different scanning speeds indicates that its stability is slightly worse.

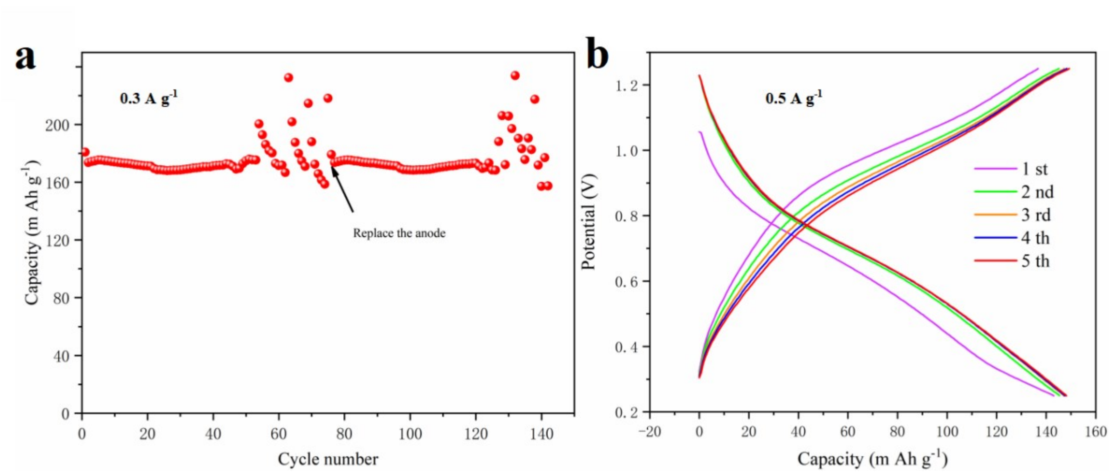

Fig. S8. (a) Cycle performance of 200-MoS_2 at low current density (0.5 A g^{-1}), (b) charge/discharge curves of 200-MoS_2 at low current density.

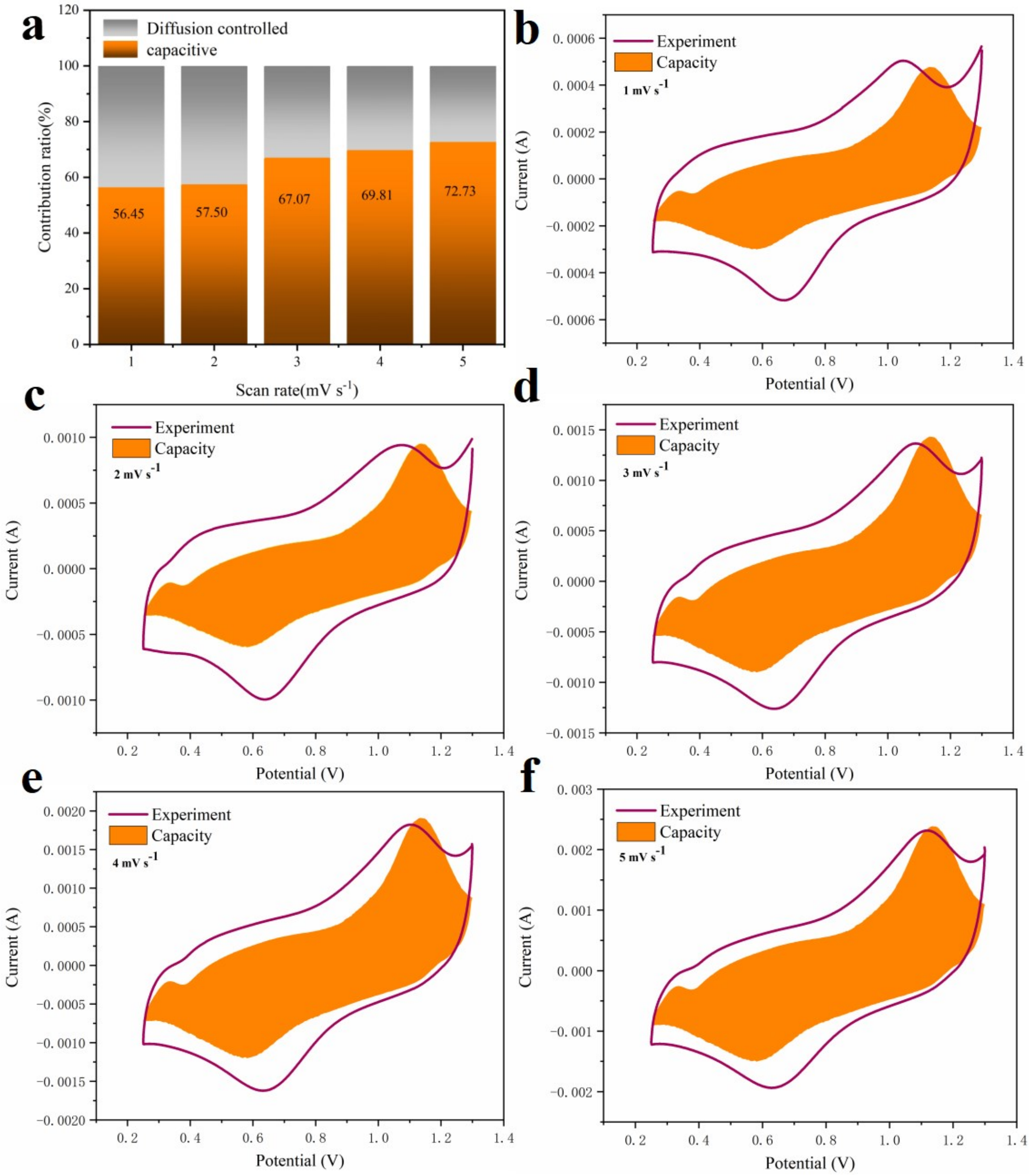

Fig. S9. 200-MoS_2 capacitive-controlled contribution calculation.

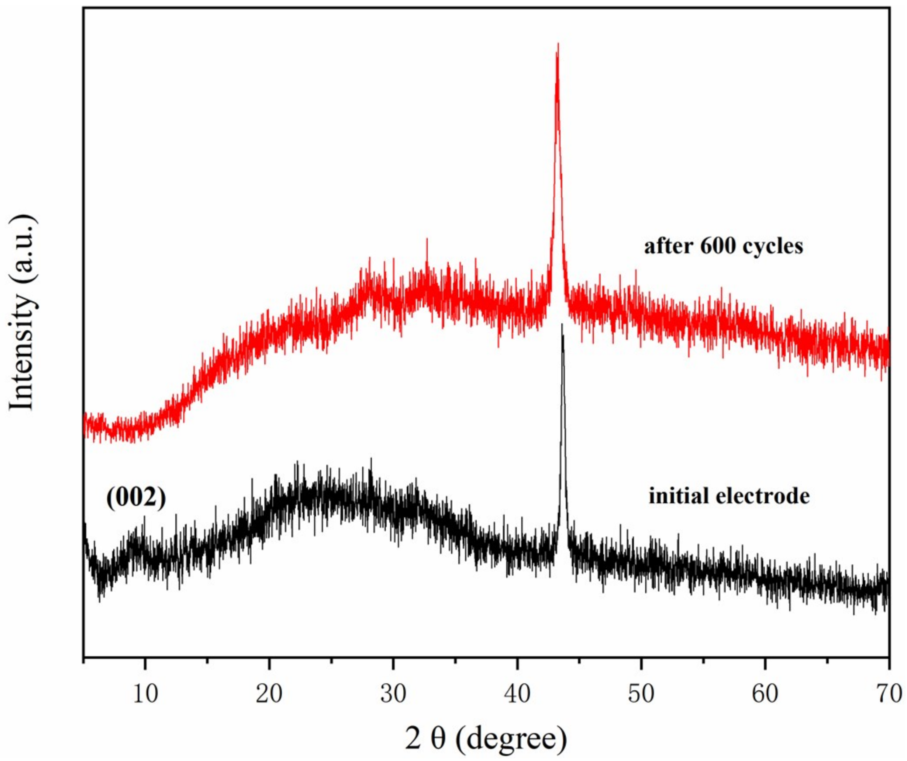

Fig. S10. XRD pattern of 200-MoS_2 electrode before and after cycling.

Table S1. data of specific surface area.

Sample	220-MoS_2	200-MoS_2	180-MoS_2
Specific surface area (m^2/g)	15.23	14.33	6.93

Table S2. Atomic percentages of MoS_2 by XPS measurement.

Atomic (%)	O 1s	S 2p	Mo 3d	N 1s	S/Mo
220	5.54	21.66	8.05	2.5	2.69
200	7.87	25.59	10.37	2.07	2.47
180	7.11	18.69	6.6	2.23	2.83

Table S3. Energy density and power density of MoS_2 at different temperatures.

	energy density (Wh kg^{-1})				power density (W kg^{-1})			
	0.5 A g^{-1}	1 A g^{-1}	2 A g^{-1}	5 A g^{-1}	0.5 A g^{-1}	1 A g^{-1}	2 A g^{-1}	5 A g^{-1}
180-MoS_2	74.93	60.41	51.74	41.75	325.47	639.29	1265.68	3088.77
200-MoS_2	100.32	87.07	77.99	66.36	331.99	674.81	1309.02	3257.61
220-MoS_2	65.70	56.13	47.3	37.14	348.05	683.32	1332.64	3261.62

Table S4. The fitting values of impedance parameters of MoS_2 at different temperatures.

Sample	R_1/Ω	R_2/Ω	R_3/Ω
220-MoS_2	5.124	4.753	411.5
200-MoS_2	4.454	44.99	337.9
180-MoS_2	3.829	64.06	437.1

Table S5. 200-MoS_2 capacitive-controlled contribution calculation results.

	1 mV s^{-1}	2 mV s^{-1}	3 mV s^{-1}	4 mV s^{-1}	5 mV s^{-1}
Experiment	0.000543075	0.00106638	0.00137118	0.00175627	0.0021075
Capacitive	0.000306563	0.000613125	0.000919688	0.00122625	0.0015328
Contribution	56.4%	57.5%	67.1%	69.8%	72.7%

Table S6. Comparison of the Zn ion storage performance of MoS_2 (in this work) and other recently reported Zn-ion battery cathodes.

Cathode material	Electrolyte	Specific capacity	Current density	Reference
MoS_2	3 M $Zn(CF_3SO_3)_2$	155 mA h g^{-1}	0.5 A g^{-1}	This work
Mo_6S_8	1 M $ZnSO_4$	60 mA h g^{-1}	60 mA g^{-1}	1
MoS_2	3 M $Zn(CF_3SO_3)_2$	134 mA h g^{-1}	0.5 A g^{-1}	2
MoS_{2-X}	3 M $Zn(CF_3SO_3)_2$	88.6 mA h g^{-1}	1 A g^{-1}	3
WS_2	2 M $ZnSO_4$	22 mA h g^{-1}	50 mA g^{-1}	4

VS_2	1 M $ZnSO_4$	190.3 mA h g^{-1}	0.05 A g^{-1}	5
VS_2 flake	1 M $ZnSO_4$	125 mA h g^{-1}	200 mA g^{-1}	6
ZnHCF	1 M $ZnSO_4$	52.5 mA h g^{-1}	300 mA g^{-1}	7
CuHCF	20 mM $ZnSO_4$	~50 mA h g^{-1}	60 mA g^{-1}	8
α-MnO_2	1 M $ZnSO_4$	210 mA h g^{-1}	21 mA g^{-1}	9
$ZnMn_2O_4$	3 M $Zn(CF_3SO_3)_2$	150 mA h g^{-1}	0.5 A g^{-1}	10
Quinones	3 M $Zn(CF_3SO_3)_2$	120 mA h g^{-1}	500 mA g^{-1}	11
Polyaniline	1 M $Zn(CF_3SO_3)_2$	82 mA h g^{-1}	5 A g^{-1}	12
$LiV_2(PO_4)_3$	4 mol kg^{-1} $Zn(CF_3SO_3)_2$	~110 mA h g^{-1}	1500 mA g^{-1}	13

References

1 Cheng, Yingwen, Luo, Langli, Zhong, Li, Chen, Junzheng and Li, Bin, Acs Applied Materials & Interfaces 2016, 8, 13673.

2 A. JL, B.PX, A. WP et al., Chemical Engineering Journal 2020, 389, 124405.

3 A. Wx et al., Energy Storage Materials 2019, 16, 527-534.

4 W. Liu, J. Hao, C. Xu, M. Jian, F. Kang, Chemical Communications, 2017, 53, 6872-6874.

5 P. He et al., Advanced Energy Materials 2017, 7, 1601920.

6 Z. Wang et al., Nano Energy 2019,56, 92-99.

7 L. Zhang, L. Chen, X. Zhou, Z. Liu, Advanced Energy Materials, 2015, 5, 1400930.

8 R. Trócoli, F. Lamantia, ChemSusChem, 2015, 8, 481-5.

9 B. Lee, S. Y. Chong, H. R. Lee, K. Y. Chung, H. O. Si, Scientific Reports, 2014, 4, 6066.

10 Ning et al., Am. Chem. Soc. 2016, 138, 12894-12901.

11 Q. Zhao, W. Huang, Z. Luo, L. Liu, L. Yong, Science Advances, 2018, 4, eaao1761.

12 F. Wan et al., Advanced Functional Materials, 2018, 28, 1804975.

13 F. Wang et al., Energy & Environmental Science, 2018, 11, 3168-3175.